Korean J. Chem. Eng., **18**(6), 831-837 (2001)

Oxidation and Reduction Characteristics of Oxygen Carrier Particles and Reaction Kinetics by Unreacted Core Model

Ho-Jung Ryu†, Dal-Hee Bae, Keun-Hee Han, Seung-Yong Lee, Gyoung-Tae Jin and Jeong-Hoo Choi*

Fluidization Research Center, Korea Institute of Energy Research, Daejeon 305-343, Korea
*Department of Chemical Engineering, Konkuk University, Seoul 143-701, Korea
(*Received 5 March 2001 • accepted 11 July 2001*)

Abstract–The reaction kinetics of the oxygen carrier particles, which are used as bed material for a fluidized bed chemical looping combustor (CLC), has been studied experimentally by a conventional thermal gravimetrical analysis technique. The weight percent of nickel and nickel oxide in oxygen carrier particles and reaction temperature were considered as experimental variables. After oxidation reaction, the pure nickel particle was sintered and unsuitable to use as fluidizing particles. The oxidation reaction rate increased with increasing weight percent of nickel in oxygen carrier particles and reaction temperature. The rate of reduction shows maximum point with weight percent of nickel oxide (57.8%) and reaction temperature (750 or 800 °C) increased. In this work, the reaction between air and Ni/bentonite particle was described by a special case of unreacted core model in which the global reaction rate is controlled by product layer diffusion resistance. However, the reaction between CH_4 and NiO/bentonite particle was described by unreacted core model in which the global reaction rate is controlled by chemical reaction resistance. The temperature dependence of the effective diffusivity of oxidation reaction and reaction rate constant of reduction reaction could be calculated from experimental data and fitted to the Arrhenius equation.

Key words: Chemical Looping Combustor (CLC), Oxidation, Reduction, Kinetics, Unreacted Core Model

INTRODUCTION

Advanced thermal power systems such as a combined cycle have been developed. However, there remain problems in these combustion systems. Fuel and air are directly mixed and burned in the conventional system. This method gives rise to some problems. One is the environmental problem about emission of carbon dioxide (CO_2), nitrogen oxides (NO_x), and so on [Park et al., 1999]. It is important to recover carbon dioxide for suppressing the greenhouse effect. One of the options to overcome greenhouse effect is the development of CO_2 capture and separation technologies from flue gases. However, most of these technologies require a large amount of energy to separate and collect CO_2 from the exhaust gas because CO_2 is diluted by N_2 in air in the conventional system. For example, if CO_2 will be recovered from the exhaust gas in power plants, it gives rise to the relative decrease of the thermal efficiency from 9 to 27% and increase in the power generation cost between 1.2 and 2.3 times [Akai et al., 1995; Kimura et al. 1995; Ishida and Jin, 1996].

To resolve these problems, Richter and Knoche [1983] proposed reversible combustion, which utilized oxidation and reductions of metal, and Ishida et al. [1987] proposed a new concept combustion method named as chemical-looping combustor (CLC).

The proposed chemical looping combustor is composed of two reactors, an oxidation reactor and a reduction reactor. Fig. 1 and formulae (1) and (2) illustrate a basic concept of a fluidized bed chemical-looping combustion (CLC) system. The system consists of a circulating fluidized bed [Kim and Han, 1999; Kim, 1999; Kim et al., 2001; Bae et al., 2001] in which oxygen carrier metal particles are recirculating between the oxidation and reduction tower.

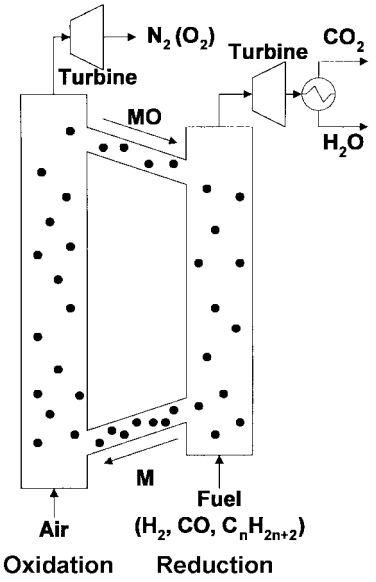

Fig. 1. Concept diagram of a chemical-looping combustor.

Oxidation reactor: exothermic reaction (800-1,300 °C)

$$M + \frac{1}{2}O_2 \rightarrow MO \quad (1)$$

†To whom correspondence should be addressed.
E-mail: hjryu@kier.re.kr
‡Presented at the Int'*l* Symp. on Chem. Eng. (Cheju, Feb. 8-10, 2001), dedicated to Prof. H. S. Chun on the occasion of his retirement from Korea University.

Reduction reactor: endothermic reaction (400-800 °C)

$$CH_4 + 4MO \rightarrow CO_2 + 2H_2O + 4M \quad (2)$$

The fuel such as CH_4, H_2, CO or C_nH_{2n+2} reacts with metallic oxide, NiO, CoO or Fe_2O_3, for example, in the reduction reactor according to formula (2), releasing water vapor and carbon dioxide from its top and metal particles (M) from its bottom. The solid product, metal particle, is transported to the oxidation reactor and reacts with oxygen in air in the oxidation reactor according to formula (1), producing high temperature flue gas and metallic oxide particles. Metallic oxide particle at high temperature is again introduced to reduction reactor and supplies the heat required for the reduction reaction. Between the two reactors, metal (or metallic oxide) performs the role of transferring oxygen and heat and, therefore, looping material (metal and metallic oxide) between the two reactors is named as oxygen carrier particle.

When reduction reaction is endothermic, heat at middle temperature (400-800 °C) is absorbed. Hence, the heat released from the oxidation reactor at high temperature (800-1,300 °C) is equal to the sum of the combustion and the heat absorbed from reduction reactor. It means that a greater amount of highlevel heat can be obtained by utilizing the middle temperature heat absorbed from reduction. This allows a higher thermal efficiency of the combustor or power plant to be obtained [Ishida and Jin, 1996].

The LNG fueled power generation system with the chemical looping combustor has the following major advantages: (a) Since the thermal efficiency of this plant may reach a new generation level, i.e., higher than 60% (based on LHV), the generation of CO_2 per kWh electricity can significantly be decreased to 0.33 kg-CO_2/kWh. (b) This combustor does not need pure oxygen, which requires high power consumption for O_2 generation, say for O_2/CO_2 combustor. (c) Since the reduction reaction produces only carbon dioxide and water vapor, CO_2 can be easily separated and collected by cooling the exhaust gas [Ishida and Jin, 1996]. (d) There is no NO_x emission because the oxidation is a gas-solid reaction between metal and air without a flame [Hatanaka et al., 1997].

The purpose of this paper is to examine the kinetics of Ni and/or NiO mixed with bentonite in the form of particles instead of powder and to clarify the effects of the various parameters such as weight percent of Ni or NiO in the oxygen carrier particles and reaction temperature. We carried out experiments to clarify the fundamental kinetics of the two reactions (oxidation and reduction) applying nickel as metal and methane as a fuel. The key points in the development of this combustor are high kinetic rates of both reaction and the life of particles that circulate between the two reactors.

EXPERIMENTAL

1. Preparation of Materials

We used nickel (Ni/bentonite) as metal in oxidation reaction and nickel oxide (NiO/bentonite) as metal oxide in reduction reaction. Pure nickel powder and bentonite powder were used to prepare the particle. Their average sizes were 1.5 and 3.9 μm, respectively.

1-1. Ni/Bentonite Particles

First, these two kinds of powder were mixed and then milled. Distilled water was added to this powder mixture, and obtained paste was dried at 105 °C for 24 hour. Dried material was crushed and dry sieve analysis was carried out. To measure the Ni weight percent in Ni/bentonite particle, particle density and porosity, EDAX and mercury porosity analysis were carried out.

1-2. NiO/Bentonite Particles

Ni/bentonite particle was calcined in the air at 900 °C for 6 hour, and dry sieve analysis was carried out. To examine the existence of nickel, which had not reacted with oxygen, XRD analysis was carried out. The particle density and porosity were measured by mercury porosimeter.

We prepared the four kinds of Ni/bentonite and NiO/bentonite specimens (particle B through E) according to the weight percent of Ni and NiO in oxygen carrier particle. The physical properties and Ni (or NiO) weight percent in Ni/bentonite (or NiO/bentonite) particles are listed in Table 1.

2. Experimental Apparatus and Methods

The reaction rates of each solid particle were measured by a TGA (thermal gravimetrical analysis) system. Fig. 2 is a schematic diagram of thermal gravimetrical analyzer apparatus (TGA 2950, TA Instrument). The temperature range, heating rate range, maximum gas flow rate, weighing range of TGA 2950 are 25-1,000 °C, 0.1-100 °C/min, 100 ml/min, 0.1 μg-100 mg or 1 μg-1,000 mg, respectively. The specimen particle was placed on a sample pan situated

Table 1. Physical properties and composition of Ni/bentonite and NiO/bentonite particles

Ni/bentonite	Ni wt%	Porosity [%]	Particle density [kg/m^3]	Bulk density [kg/m^3]
Particle B	21.6	68.1	2655	847
Particle C	37.9	68.2	2962	941
Particle D	51.9	77.5	5197	1170
Particle E	74.0	79.5	7374	1515
NiO/bentonite	**NiO wt%**	**Porosity [%]**	**Particle density [g/cm^3]**	**Bulk density [g/cm^3]**
Particle B	26.0	71.4	3562	1020
Particle C	43.7	71.3	3629	1043
Particle D	57.8	64.5	3589	1273
Particle E	78.4	59.0	3731	1530

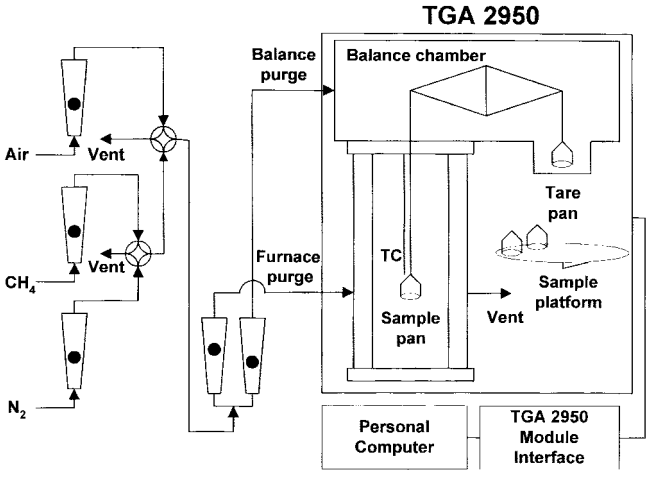

Fig. 2. Schematic diagram of TGA reactor.

Table 2. Summary of experimental methods and variables

Reaction	Oxidation	Reduction
Particles	Ni/Bentonite	NiO/Bentonite
Method	Isothermal	Isothermal
Inert gas	N_2	N_2
Reacting gas	Air (100 ml/min)	CH_4 (5.04%, 100 ml/min)
Experimental variables		
Ni or NiO content	Particle B, C, D, E	Particle B, C, D, E
Temperature [°C]	850, 900, 950, 1000	650, 700, 750, 800, 850, 900

on the sample arm of the balance. The reactant gas (Air for oxidation and CH_4 for reduction), which was controlled by float type flowmeter, was introduced into the reaction unit. Inert gas (N_2) was fed into the weighing unit to prevent the reactant gas from diffusing into the balance chamber. When the temperature reached the specified value by use of an electric furnace, four-port switching valves changed the gaseous stream from nitrogen to reactant. The weight of the solid particle and the reaction temperature were recorded continuously by a computer. In all experiments the flow rates of the reactant gas (Air or CH_4) and inert gas (N_2) were set as 100 ml/min (at standard state) to make the effect of gas film diffusion negligibly small.

The weight percent of Ni or NiO in the oxygen carrier particles and reaction temperature were considered as experimental variables. Experimental methods and variables are summarized in Table 2.

RESULTS AND DISCUSSION

1. Oxidation Reaction

Fig. 3 shows the oxidation reaction results of Ni/bentonite particles of 80 μm in diameter according to the weight percent of nickel in the oxygen carrier particles. The oxidation experiments were performed at 900 °C. The oxidation conversion X is plotted against the reaction time, where X is defined as $X=(W-W_{Ni})/(W_{NiO}-W_{Ni})$, where W is instantaneous weight and W_{Ni} and W_{NiO} are the completely reduced weight (initial weight) and completely oxidized weight, respectively. Therefore, X=1 corresponds to completely oxidized state (NiO/bentonite), while X=0 to completely reduced state (Ni/bentonite). A significant effect of Ni content on the oxidation rate is seen in Fig. 3 for different contests of Ni: 21.6, 37.9, 51.9, 74.0%. Completely different behaviors were observed, and the oxidation rate depended strongly on the Ni content. As can be seen in Fig. 3, the oxidation rate increased with increasing the nickel weight percent (E>D>C>B). For 74.0% Ni content, we found a satisfactorily high oxidation rate. The explanation is that the particle E has larger porosity (larger surface area) than other particles over which the reaction can take place, smaller diffusion resistances of O_2 through the product layer and gas film. For pure nickel particles, the nickel particle was sintered and unsuitable to use as fluidizing particles.

The effect of the reaction temperature was examined for Ni/bentonite particle E of 80 μm in diameter. The results are shown in Fig. 4. It was found that the oxidation rate is strongly dependent on temperature, and increased with increasing the reaction temperature. As expected, the reaction rates are low at low temperature because of reaction rate constant.

2. Reduction Reaction

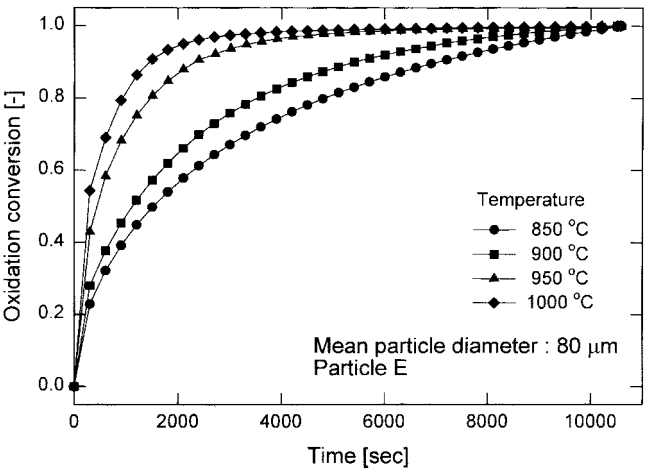

Fig. 4. Effect of reaction temperature on oxidation reaction of Ni/bentonite particle.

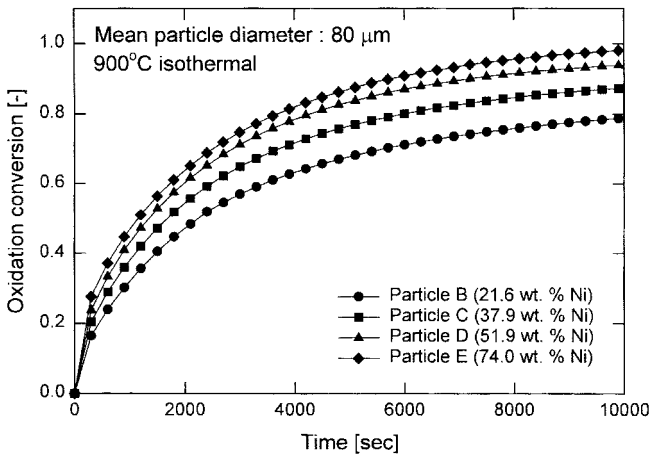

Fig. 3. Effect of Ni weight percent in Ni/bentonite particle on oxidation reaction.

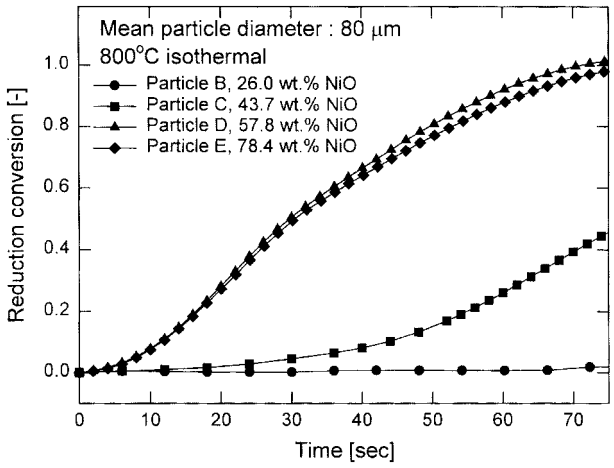

Fig. 5. Effect of NiO weight percent in NiO/bentonite particle on reduction reaction.

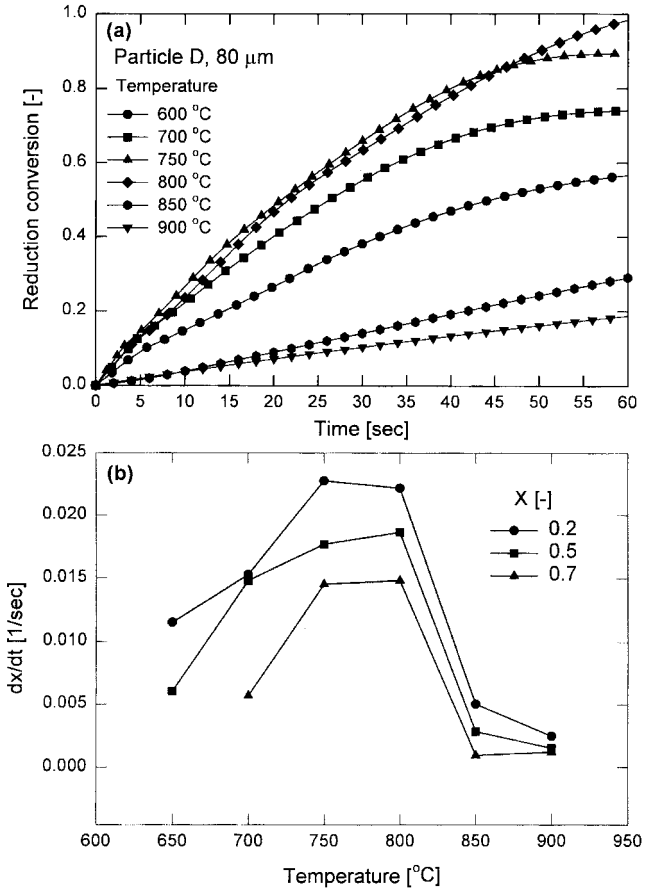

Fig. 6. Effect of reaction temperature on reduction reaction of NiO/bentonite particle.

Fig. 5 shows the reduction reaction results of NiO/bentonite particles of 80 μm in diameter according to the weight percent of nickel oxide in the oxygen carrier particle. The reaction temperature was 800 °C. The reduction conversion X is plotted against the reaction time, where X is defined as $X=(W_{NiO}-W)/(W_{NiO}-W_{Ni})$. As can be seen in Fig. 5, the reduction rate of particle D was faster than that of particle B, C, and E. The explanation is that the particle D has larger porosity (larger surface area) than particle E over which the reaction can take place, smaller diffusion resistances of CH_4 through the product layer and gas film.

Fig. 6(a) shows the dependence of reaction temperature on reduction rate of NiO/bentonite D particle. The particles tested were 80 μm in diameter. The reduction rate increased as the reaction temperature increased from 600 to 800 °C. At high temperature (850 and 900 °C), the reduction rate decreased as temperature increased. Fig. 6(b) shows the reduction rates at three different reduction conversions, X=0.2, 0.5 and 0.7. The reduction rate exhibits maximum value as reaction temperature increases. The reduction rate at X=0.2 shows maximum value at 750 °C. However, the reduction rates at X=0.5 and 0.7 show maximum value at 800 °C.

3. Interpretation by Macroscopic Reaction Model

The unreacted-core model was applied to interpret the above experimental results for Ni/bentonite particle E (for oxidation reaction) and NiO/bentonite particle D (for reduction reaction). The unreacted core model requires that the reaction be confined to surface separating the solid reactant core from outer product layer. The initial reaction surface corresponds to the external surface of the solid. The thickness of the product layer increases with time, producing a shrinking core of unreacted solid. Within the core of solid reactant, the concentration is unchanged from its initial value of C_{B0}, while the solid reactant concentration within the product layer is zero. The general gas-solid reaction can be represented by the following stoichiometry:

$$A(g)+bB(s)\rightarrow \text{Product} \tag{3}$$

For the Ni/bentonite and NiO/bentonite particle, the specific reaction is

$$O_2(g)+2Ni\rightarrow 2NiO \tag{4}$$

$$CH_4(g)+4NiO\rightarrow CO_2+2H_2O+4Ni \tag{5}$$

The following assumptions are made [Marban et al., 1999]:

- The porosity of the oxygen carrier particles is neglected.
- The particles are spherical.
- There is no influence of external mass transfer on the reaction.
- The reaction is first order with respect to the concentration of reactant gas.
- The particle volume is constant during reaction because of the physical strength of bentonite.
- The reaction is isothermal and at pseudo-steady state condition.

With these hypotheses the following conversion-time expression for the reaction of Ni/bentonite(and/or NiO/bentonite) particles are obtained [Szekely et al., 1976; Na et al., 1999; Qui et al., 1997; Kang et al., 1997]:

$$t=t_c+t_d \tag{6}$$

where

$$t_c=\frac{C_{B0}R_p}{bkC_{A0}}[1-(1-X)^{1/3}] \tag{7}$$

$$t_d=\frac{C_{B0}R_p^2}{6bD_eC_{A0}}[1-3(1-X)^{2/3}+2(1-X)] \tag{8}$$

t is the elapsed time to achieve a conversion x, t_c is the time necessary to get the same conversion under chemical reaction control and t_d represents the time under product layer diffusion control. The initial concentration of the solid reactant (C_{B0}) is given as follows [Shin, 1990]:

$$C_{B0}=\frac{w_0(1-\varepsilon)}{M_B\left[\frac{w_0}{\rho_B}+\frac{(1-w_0)}{\rho_N}\right]} \tag{10}$$

where w_0 is the initial weight fraction of Ni (or NiO) in Ni/bentonite (or NiO/bentonite) particle, ε the porosity of solid, M_B the molecular weight of Ni (or NiO), ρ_B density of Ni (or NiO), and ρ_N the density of bentonite.

The reaction rate control resistances of oxidation and reduction of oxygen carrier particles were quite different because the extent of penetration and diffusion of reactant gas through the Ni or NiO layer was different. The layer of NiO was denser than that of Ni [Hatanaka et al., 1997]. At the early reaction stage, CH_4 performs

the role of removing the dense layer of NiO, i.e., the outer skin from the metal particle. And thereafter, CH_4 can easily enter into the inside through the loose layer of Ni and react with internal metal oxide as can be seen in Fig. 7. However, in the oxidation reaction, the thickness of dense NiO layer increases with time. Penetration and diffusion of O_2 through the dense NiO layer is difficult (Fig. 7). Therefore, in this work, we assumed oxidation reaction is product layer diffusion control and reduction reaction is chemical reaction control.

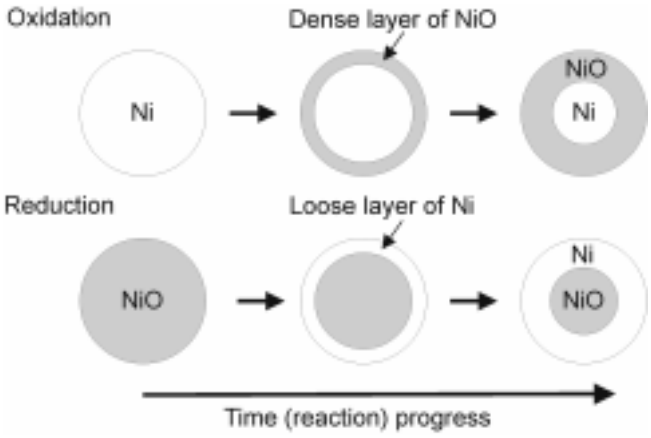

Fig. 7. Illustration of a reacting particle at oxidation and reduction.

Fig. 8 shows results simulated by a special case of unreacted core model in which the global reaction rate is controlled by product layer diffusion resistance. The lines in Fig. 8(a) represent the curve simulated for base case of Ni/bentonite particle E for oxidation reaction, where the effective diffusion coefficient D_e was chosen to best fit the observed data shown by symbols. It is found for the oxidation reaction that the curve obtained by the product layer diffusion

Table 3. Summary of determined effective diffusion coefficients and chemical reaction rate constants by unreacted core model

Oxidation		Reduction	
Temperature [°C]	D_e [m²/s]	Temperature [°C]	k [m/s]
850	1.436×10^{-11}	600	2.030×10^{-4}
900	1.920×10^{-11}	700	3.140×10^{-4}
950	4.548×10^{-11}	750	4.408×10^{-4}
1,000	7.012×10^{-11}		

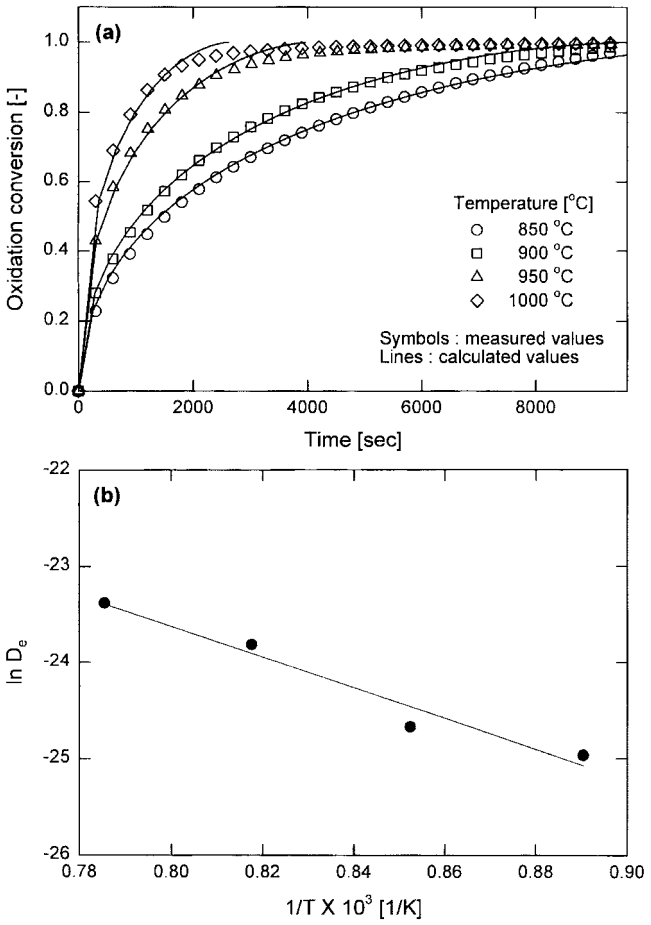

Fig. 8. Results of unreacted core model for oxidation reaction of Ni/bentonite particle (product layer diffusion control).
(a) Comparison of calculated conversion curves by unreacted core model with the experimental data. (b) Temperature dependence of the effective diffusion coefficients.

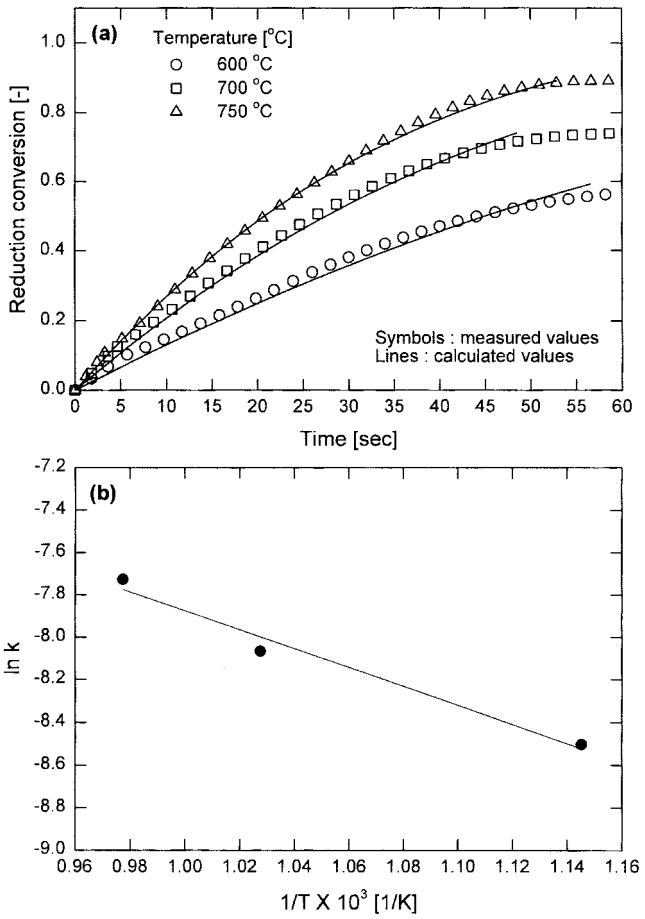

Fig. 9. Results of unreacted core model for reduction reaction of NiO/bentonite (chemical reaction control).
(a) Comparison of calculated conversion curves by unreacted core model with the experimental data. (b) Temperature dependence of the chemical reaction rate constants.

control model simulates reasonably well the experimental results. The obtained values of D_e are shown in Table 3 and reasonably well fitted to the Arrhenius equation, as can be seen in Fig. 8(b). A fitting of D_e with temperature shown in Fig. 8(b) permits to express the effective diffusivity as a function of temperature by means of following equation:

$$D_e = 1.76\times10^{-5}\exp\left(-\frac{31454.2}{RT}\right)\ [m^2/s] \qquad r^2=0.98 \qquad (11)$$

Fig. 9(a) shows results simulated by a special case of unreacted core model in which the global reaction rate is controlled by chemical reaction resistance. The lines in Fig. 9(a) represent the curve simulated for base case of Ni/bentonite particle D for reduction reaction. The rate constant for chemical reaction k was chosen to best fit the observed data shown by symbols. It is found for the reduction reaction that the curve obtained by the chemical reaction control model simulates reasonably well the experimental results. The obtained values of k are also shown in Table (3) and reasonably well fitted to the Arrhenius equation, as can be seen in Fig. 9(b). A fitting of k with temperature shown in Fig. 9(b) permits one to express the chemical reaction rate constant as a function of temperature by means of the following equation:

$$k = 3.27\times10^{-2}\exp\left(-\frac{8854.1}{RT}\right)\ [m/s] \qquad r^2=0.98 \qquad (12)$$

Based on the comparison between experimental data and model, the oxidation reaction is controlled by product layer diffusion resistance and reduction reaction is controlled by chemical reaction resistance.

CONCLUSIONS

The oxidation reaction rate increased with increasing weight percent of nickel in oxygen carrier particles and reaction temperature. The rate of reduction shows maximum point with weight percent of nickel oxide and reaction temperature increased. Based on the comparison between experimental data and model, the oxidation reaction is controlled by product layer diffusion resistance and reduction reaction is controlled by chemical reaction resistance. Temperature dependence of the effective diffusivity of oxidation reaction and reaction rate constant of reduction reaction could be calculated from experimental data and can be fitted to the Arrhenius equation as follows:

$$D_e = 1.76\times10^{-5}\exp\left(-\frac{31454.2}{RT}\right)\ [m^2/s]$$

$$k = 3.27\times10^{-2}\exp\left(-\frac{8854.1}{RT}\right)\ [m/s]$$

NOMENCLATURE

A(g) : gas reactant
B(s) : solid reactant
b : stoichiometric coefficient of reaction
C_{A0} : bulk concentration of gaseous reactant [kg-mol/m^3]
C_{B0} : initial concentration of the solid reactant [kg-mol/m^3]
D_e : effective diffusion coefficient [m^2/s]
k : chemical reaction rate constant [m/s]
k_{mA} : mass transfer coefficient [m/s]
M_B : molecular weight of Ni (or NiO) [kg/kg-mol]
R : gas constant, 1.987 [Kcal/kg-mol K]
R_p : radius of particle [m]
T : absolute temperature [K]
t : time [sec]
t_c : time necessary to get the conversion x under chemical reaction control [sec]
t_d : time necessary to get the conversion x under product layer diffusion control [sec]
W : instantaneous weight of particles [mg]
W_{Ni} : completely reduced weight of particles [mg]
W_{NiO} : completely oxidized weight of particles [mg]
w_0 : initial weight fraction of Ni (or NiO) in Ni/bentonite (or NiO/bentonite) particle [-]
X : conversion [-]

Greek Letters

ε : porosity of solid [-]
ρ_B : density of Ni (or NiO) [kg/m^3]
ρ_N : density of bentonite [kg/m^3]

REFERENCES

Akai, M., Kagajo, T. and Inoue, M., "Performance Evaluation of Fossil Power Plant with CO_2 Recovery and Sequestering System," *Energy Convers. Mgmt*, **36**, 801 (1995).

Bae, D. H., Ryu, H. J., Shun, D., Jin, G. T. and Lee, D. K., "Effect of Temperature on Transition Velocity from Turbulent Fluidization to Fast Fluidization in a Gas Fluidized Bed," *HWAHAK KONGHAK*, **39**, 456 (2001).

Cho, S. G., Lee, J. Y., Lee, S. W. and Lee, K. H., "Oxidation of Nickel in the Temperature Range of 800 °C to 1,200 °C at Air," *J. of the Korean Inst. of Met. and Mater.*, **30**(3), 278 (1992).

Hatanaka, T., Matsuda, S. and Hatano, H., "A New-Concept Gas-Solid Combustion System "MERIT" For High Combustion Efficiency and Low Emissions," Proceedings of the Thirty Second IECEC, **1**, 944 (1997).

Ishida, M. and Jin, H., "A Novel Chemical-Looping Combustor without NO_x Formation," *Ind. Eng. Chem. Res.*, **35**, 2469 (1996).

Ishida, M. and Jin, H., "CO_2 Recovery in a Power Plant With Chemical Looping Combustion," *Energy Convers. Mgmt.*, **38**, S187 (1996).

Ishida, M., Zheng, D. and Akehata, T., "Evaluation of a Chemical-Looping Combustion Power-Generation System by Graphical Exergy Analysis," *Energy-The Int. Journal*, **12**, 147 (1987).

Kang, S. H., Rhee, Y. W., Kang Y., Han, K. H., Yi, C. K. and Jin, G. T., "A Study of Desulfurization Reaction Using Zinc Titanate at High-Temperature," *HWAHAK KONGHAK*, **35**, 642 (1997).

Kim, J., "Hydrodynamics Behavior of Solid Transport for a Closed Loop Circulating Fluidized Bed with Secondary Air Injection," *Korean J. Chem. Eng.*, **16**, 840 (1999).

Kim, S. H. and Han, G. Y., "An Analysis of Pressure Drop Fluctuation in a Circulating Fluidized Bed," *Korean J. Chem. Eng.*, **16**, 677 (1999).

Kim, S. W., Ahn, J. Y., Lee, D. H. and Kim, S. D., "Continuous Measurement of Solids Flow in a Circulating Fluidized Bed," *Korean J.*

Chem. Eng., **18**, 555 (2001).
Kimura, N., Omata, K., Kiga, T., Takano, S. and Shikisma, S., "The Characteristics of Pulverized Coal Combustion in O_2/CO_2 Mixture for CO_2 Recovery," *Energy Convers. Mgmt*., **36**, 805 (1995).
Marban, G., Garcia-Calzada, M. and Fuertes, A. B., "Kinetics of Oxidation of CaS Particles in the Regime of Low SO_2 Release," *Chem. Eng. Sci.*, **54**, 77 (1999).
Na, J. I., Park, S. J., Wi, Y. H., Yi, C. K. and Lee, T. J., "Sulfidation Reactivity of Zinc Titanate Sorbent and Reaction Kinetics by Unreacted Core Model," *HWAHAK KONGHAK*, **37**, 499 (1999).
Park, J. H., Kim, Jaehun, Cho, S. H., Han, K. H., Yi, C. K. and Jin, G. T., "Development of Sorbent Manufacturing Technology by Agitation Fluidized Bed Granulator (AFBG)," *Korean J. Chem Eng*., **16**, 659 (1999).
Qui, K., Mattisson, T., Steenari, B.-M. and Lindqvist, O., "Thermogravimetric Combined with Mass Spectrometric Studies on the Oxidation of Calcium Sulfide," *Thermochimica Acta*, **298**, 87 (1997).
Richter, H. J. and Knoche, K. F., "Reversibility of Combustion Process," *ACS Symposium Series*, R. A. Gaggioli, ed., Washington, D. C., **235**, 71 (1983).
Shin, C. S., "Simultaneous Removal of SO_2 and NO by Using Metal Oxide," Research Report, 893-1002-016-1 (1990).
Szekely, J., Evans, J. W. and Sohn, H. Y., "Gas-Solid Reaction," Academic Press, New York (1976).